Variety Management in Manufacturing. Proceedings of the 47th CIRP Conference on Manufacturing Systems

Applying neural network based on fuzzy cluster pre-processing to thermal error modeling for coordinate boring machine

J.Yang*, H. Shi, B.Feng, L.Zhao, C.Ma, X. Mei

State Key Laboratory for Manufacturing Systems Engineering, Xi'an Jiaotong Univeristy, No.28 Xianning West Road, Xi'an 710049, P.R.China

* Corresponding author. Tel.: +86-29-8266-3870; fax: +86-29-8266-8604. *E-mail address:* softyj@163.com

Abstract

To investigate the effect of the thermal characteristics of a motorized spindle system on the precision of a machine tool, a thermal error model for spindle axial expansion and radial thermal declination is proposed. With precision CNC coordinate boring machine as an object, using the five-point method to calibrate spindle system thermal errors by the eddy current sensors for axial thermal elongation and radial thermal tilted values, and temperatures of measurement points are obtained by the PT100. The relationships between the rotational speed and temperature field, thermal errors are analyzed. Then fuzzy clustering analysis method is used to group and optimize the temperature variables, selecting the variables for thermal error-sensitive. Finally the MIMO artificial neural network approach is established for the spindle axial thermal elongation and radial thermal drifts. The results indicated that the model prediction accuracy could reach 86% with perfect generalization ability under different cutting conditions, providing a theoretical model and thermal characteristic parameters for both thermal error compensation and thermal equilibrium design.

1. Introduction

Precision CNC coordinate boring machine is a tool for processing complex box-type components. However, the accuracy decreases and becomes far lower than the initial design value after the machine is used for a long period of time. This decreased accuracy over time primarily results from inadequate maintenance and accuracy stability, and the thermal error is the main factor for the inadequate accuracy, accounting for 70% of the total number of errors arising from various error sources [1]. Thermal error will account for a larger proportion of total error as the machine tools become more sophisticated. Moreover, the dynamical characteristic of a spindle also affects the thermal error; Zhang Yun proposed a holospectrum-based balancing method to improve the machining accuracy [2]. A non-uniform temperature distribution causes thermal errors in CNC machine tools; this

distribution becomes non-linear and non-stationary and varies with time. The mutual coupling of location and strength of the heat source, coefficient of expansion, and machine structure create complex thermal characteristics [3]. Donmez proposed that changing temperatures produce thermal error and thermal error is a major factor for reducing machine precision [4].

In recent years, the finite element method (FEM), which is used to analyze temperature fields and thermal deformation of machine tools, has become a topic of increasing interest, where Min established a variety of thermal boundary conditions for a thermal state model based on the Fourier thermodynamic equation and analyzed the gradient distribution of the screw temperature field under different heat fluxes [5]. Zhao proposed a method for calculating thermal conductivity coefficient of the spindle surface, and simulated and analyzed variation principles of temperature field and thermal deformation of the spindle [6]. Creighton used the

finite element method to analyze temperature distribution characteristics for high-speed micro-milling spindle, and constructed an exponential model of axial thermal error related with the spindle speed and running time [7]. However, precision CNC machine tool error is a mutual coupling of many complex factors that are affected by many variables, and therefore, it is extremely difficult to establish a theoretical equation from the perspective of thermo elasticity and heat transfer.

Neural Network can describe nonlinear mappings relationship very well. Since Rumelhart proposed learning methods of multilayer back propagation [8], many scholars have begun to apply neural network to thermal error modeling. Chen and Yang [9, 10] used artificial neural networks (ANNS) to establish a relationship between temperature and the thermal error of a spindle, and the model was useful for making generalizations. Zhang integrated gray system model and artificial neural network model to establish a gray neural network model, and the model has better predictive ability than the traditional neural network model [11]. Ouafi constructed an artificial neural network model for spindle thermal error with the temperature drawing on statistical methodology, and carried out the error compensation experiments, which effectively improves the machining accuracy [12]. Hong studied thermal characteristics of a rotary axis on the five-axis machine, and analyzed effect of thermal error on errors motion of the rotary axis, then calculated how errors motion of the rotary axis can be affected by the thermal error with the help of geometric errors [13]. Vyroubal presents a method focused on compensation of machine's thermal deformation in spindle axis direction based on decomposition analysis, which is cheap and effective strategy [14]. Vissiere measures spindle thermal drifts with a new method which measurement accuracy can reach even to the nanometer [15].

The current study focuses on a spindle system of a box-type precision CNC coordinate boring machine. Thermal balance experiments were performed using a temperature displacement acquisition system to measure the distribution of the temperature field and thermal deformation at different spindle speeds. The study analyzes how different spindle speeds affect thermal characteristics, then using fuzzy clustering regression analysis method to optimize the temperature variables, selected the variables for thermal error-sensitive, finally the MIMO artificial neural network approaches were established for spindle axial thermal elongation and radial thermal tilts. Subsequently, a new set of sample data is used to validate the model. The results indicate that the model has high prediction accuracy with perfect generalizations; one can obtain an exact model for subsequent thermal error compensation that provides references for the characteristic parameter for thermal equilibrium.

2. Experimental principles and equipment

2.1 Experimental system

The experimental system is shown in Figure 1, which focuses on the spindle of precision CNC coordinate boring machine. The system analyzes the change in the temperature field and the thermal distortion of the spindle system. The maximum speed of spindle is N = 20000rpm, and the cooling system for the spindle is controlled intelligently by temperature. Front and rear bearings and motor were cooled respectively.

The measuring equipment and functions are as follows: a synchronous acquisition system (developed by our group with *NI SCXI* as its structural base) is used to determine the temperature and thermal deformation. This system uses *Pt*100 precision magnetic temperature sensors to measure the temperature for the spindle system motor, bearings, pedestal, coolant, and environment. High-precision eddy-current sensors are applied to measure the spindle thermal drifts. The system carries out real-time synchronous acquisition of temperature and thermal drifts.

Fig.1. Experimental setup

Table 1 presents and describes the machine positions of the magnetic temperature sensors (*PT*100), denoted T_1… T_{11}, and the eddy-current displacement sensors S_1... S_5.

Table 1. Temperature sensor and displacement sensor mounting position

Temperature sensor / displacement sensor	Installation location
T1	rear bearing
T2	spindle base
T3	rear bearing cooling out
T4	front bearing cooling out
T5	ambient temperature
T6	front bearing oriented X-
T7	front bearing oriented Y+
T8	motor oriented Y+
T9	the cooling in
T10	motor cooling out
T11	motor oriented X-
S1	radial near X-axis
S2	radial near Y-axis
S3	radial distal X-axis
S4	radial distal Y-axis
S5	Z axial direction

2.2. Measuring principle

The spindle thermal drifts are measured by using a five-point method [16], a displacement sensor fixture and measurement diagram are shown in Figure 2. The spindle is parallel to Z-axis, and the axial thermal expansion can be

obtained by the S_5. The radial thermal yaw θ_x partial X direction is measured by the S_1、S_3, and the radial thermal pitch θ_y partial Y direction is measured by the S_2、S_4. The acquisition system recorded the data once every 1s.
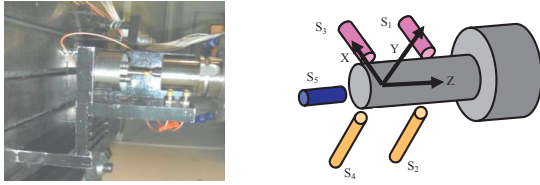

Fig. 2. (a) The displacement sensor fixture (b) five point's measurement sketch map

After the spindle running for a long period, the thermal elongation expanded to axial direction and thermal angle inclined to radial direction, resulting from the uneven temperature gradient distribution, which is shown in Figure 3, and the thermal yaw angle is:

$$\Delta L_3 = L_3^i - L_3^0 \tag{1}$$

$$\Delta L_1 = L_1^i - L_1^0 \tag{2}$$

$$\Delta L = \Delta L_3 - \Delta L_1 \tag{3}$$

$$\tan\theta_x = \frac{\Delta L}{D} \tag{4}$$

Where i denotes the number of measurements. The thermal yaw angle is too small in this experiment, that is $\theta_x \to 0$, so:

$$\theta_x \sim \tan\theta_x \tag{5}$$

As shown in Equation (6), the thermal yaw can be obtained by applying Equations (1)-(5).

$$\theta_x = \frac{(L_3^i - L_1^i) - (L_3^0 - L_1^0)}{D} \tag{6}$$

Where L_3^0 and L_1^0 is the radial displacement between the sensor probe and the spindle measured by S3, S1 respectively in the initial state, L_3^i and L_1^i is the transient displacement during the running operation. D is the distance between S_1 and S_3, S_2 and S_4, and D=120mm.

Similarly, the thermal pitch angle in the Y direction can be obtained:

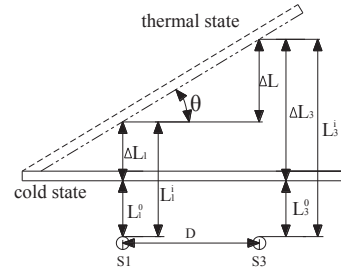$$\theta_y = \frac{(L_4^i - L_2^i) - (L_4^0 - L_2^0)}{D} \tag{7}$$

Fig. 3. The spindle thermal inclination sketch

3. Experimental results and analysis

The spindle speed affects the temperature field distribution and the magnitude of thermal drifts. This section focuses on a set of experimental data. In order to simulate the actual spindle speed changes during processing, the velocity varies in the experiment, and the specific speed distribution is shown in Figure 4.
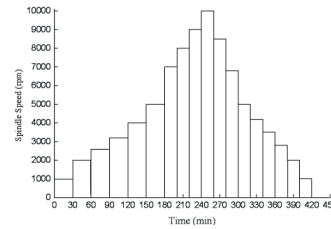

Fig. 4. Step Speeds distribution

3.1. Temperature distribution

The spindle system temperatures variations are shown in Figure 5. The overall temperatures trend of all the measuring points increases with time, but the general increase in temperature exhibits cyclical changes with a cycle time. This is because temperatures of the spindle system were controlled by intelligent cooling system, which sets a temperature threshold value and starts to reduce the temperature when the component temperature is higher than this threshold value. Therefore, the increase in temperature exhibits fluctuations changes.

The front bearing, rear bearing and the motor are cooled separately in the cooling processing, but when they are cooling, temperatures will be inhibited to increase and the cooling fluid takes away an amount of heat energy which is less than the heat generated by the spindle, so the overall trend is still increasing. And it takes approximately 320min for temperature to reach thermal equilibrium, and then the rear bearing has the highest temperature reaching 32 ℃ due to large capacity, heavy load, severe friction which generates more heat, and followed by the motor whose temperature is 27.3 ℃. Temperatures of the other measuring points are about 26 ℃. The ambient temperature T_5 increased from 21.3℃ to 23.8℃.
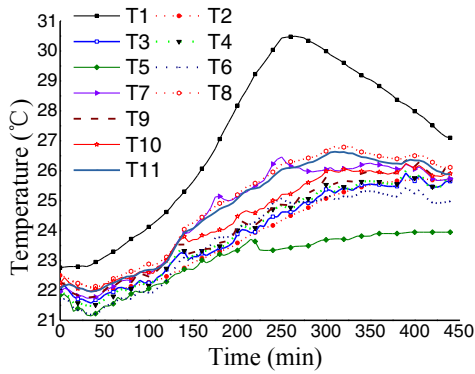
Fig. 5. Temperatures of the spindle

3.2. Variation of thermal drifts

Figure 6 presents the spindle thermal drifts. The measurements taken from the points in Figure 6 indicate that the displacement trends are gradually increased over time, eventually reaching thermal equilibrium. Z-axis axial thermal elongation increases as time increases, and the direction is negative, which indicates that the spindle thermal expansion to the negative direction on Z–axis. The time until equilibrium is reached is approximately 385 min, with a maximum elongation of 39.6μm. The thermal error on X-axis direction is positive, which indicates that during the heating process, the spindle is away from the displacement sensors S_1/S_3, it deviates from the Z axis, the spindle swings to the negative direction in the X axis on the XZ plane, and its thermal yaw angle to the Z axis is θ_x, the maximum amount of hot offset error is 35μm. Thermal error in Y direction is negative which indicates during operation the spindle is closer to the displacement sensors S_2/S_4, and it deviates from the Z-axis, and the spindle in the YZ plane pitches to the negative direction on the Y–axis, and and its thermal pitch angle to the Z axis is θ_y, the maximum thermal offset is of 20.2μm.
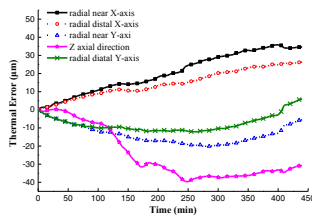

Fig. 6 Thermal drifts of the spindle

4. Fuzzy clustering grouping and optimization for temperature measuring points

Famous scholar Ruspini [17] was the first to propose the concept of fuzzy partition, he introduced the fuzzy set theory into cluster analysis, then, other researchers have presented a variety of fuzzy clustering analysis method based on fuzzy graph theory, among which include the biggest tree method based on Fuzzy Graph Theory [18]. This paper groups temperature variables of 11 measuring points using the fuzzy

clustering, and then applies statistical correlation to optimize the measuring points and calculated correlation coefficient between each variable temperature and thermal error, finally, take the measuring points whose correlation coefficient is bigger in each group as the typical temperature variables.

4.1. Hierarchical clustering method

As the temperature variables are in small quantities, so we use system cluster analysis, and the variable packet process is shown in Figure 7.
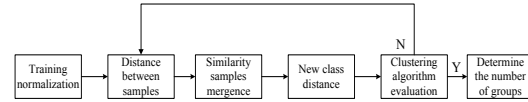

Fig. 7. Fuzzy Clustering Grouping

Assume the temperature variable $T= \{T_1, T_2... T_m\}$ is the object to be carried out by a fuzzy clustering analysis. Each object in T is T_k (k=1, 2... m) whose characteristics can be described by a limited number of values. Therefore there is a corresponding vector $P(T_k)=(T_{k1}, T_{k2},..., T_{ks})$ to the object T_k. T_{kj}(j=1,2,...,s) is the jth characteristics value of T_k. $P(T_k)$ is the eigenvectors for T_k. Fuzzy clustering analysis is to divide sample T into c fuzzy subsets $\bar{T}_1, \bar{T}_2,...,\bar{T}_c$, according to the similarity between the feature vectors.

Cluster Analysis, also known as hierarchical clustering analysis method, is to gradually cluster according to feature vector distance criteria. The classification moves from more to less, until reaches the desired classification. The following are the general steps for system clustering:

1. Initialize the data. Assuming that T sample set contain m subsets $T_1^{(0)}$, $T_2^{(0)}$, ,..., $T_m^{(0)}$, which form one class, then calculate distance between each subset, and obtain $m \times m$ dimensional distance matrix $D^{(b)}$;

2. Find the smallest element in the distance matrix $D^{(b)}$ (except diagonal elements) , if the minimum element is the distance between $T_i^{(b)}$ and $T_j^{(b)}$, and then the two will be merged into $T_{ij}^{(b+1)}$ .Finally, get a new classification $T_1^{(b+1)}$, $T_2^{(b+1)}$, ,..., $T_{m-1}^{(b+1)}$;

3. Computing distances between the new categories after merging cluster to get the distance matrix $D^{(b+1)}$;

4. Repeat the second step of the work until the classification meets the requirements.

m=11, set the number of packets C=4, after calculating, combination of Euclidean-centroid clustering algorithm obtained the optimal grouping, the cluster groupings are shown in Figure 8, divide the temperature variables into Groups $\{T_1\},\{T_5\},\{T_2, T_3 ,T_4, T_6 ,T_9 ,T_{10}\},\{T_7, T_8 ,T_{11}\}$.
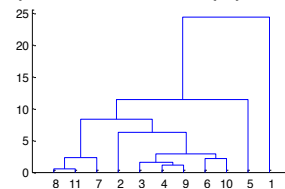

Fig. 8. Clustering dendrogram

4.2. Optimization of temperature variables

Based on the results above the groups, correlation coefficients between axial thermal error E and the temperature Ti can be calculated:

$$\rho_{T_i E} = \frac{\sum_{j=1}^{n}\left(T_{ij}-\overline{T_i}\right)\left(E_j-\overline{E_j}\right)}{\sqrt{\sum_{j=1}^{n}\left(T_{ij}-\overline{T_i}\right)^2}\sqrt{\sum_{j=1}^{n}\left(E_j-\overline{E_j}\right)^2}} \qquad (8)$$

In the equation, $i=1, 2...m$, as the temperature measurement points. $j=1, 2... n$, as the number of measurements. T_{ij} is the temperature of measuring point; E_j is the thermal elongation, $\overline{T_i}$ is the average temperature of ith measurement point, $\overline{E_j}$ is the average thermal elongation. Correlation coefficients are shown in Table 2. Selecting the temperature variable whose coefficient is higher as a typical variable in each cluster. T_{10} is the outlet liquid temperature of motor coolant, and its temperature has more significant influence to motor temperature, so it is reserved as a key variable, finally we choose T_1, T_5, T_6, T_7 and T_{10} as the typical temperature variables.

Table 2. Correlation Coefficients between Temperature and Axial Thermal error

Temperature	Cluster	ρ	Temperature	Cluster	ρ
T_1	4	0.9651	T_7	1	0.9902
T_2	2	0.8593	T_8	1	0.9739
T_3	2	0.9054	T_9	2	0.8948
T_4	2	0.9242	T_{10}	2	0.9344
T_5	3	0.9546	T_{11}	1	09737
T_6	2	0.9706			

5. MIMO neural network modeling

The relationship between spindle thermal errors and temperatures is strong nonlinear. A multi-input multi-output spindle thermal error model was established based on feedback neural network (Back Propagation).

$$P = \psi(T) \qquad (9)$$

Where $P = (E, \theta_x, \theta_y)$ is an output vector of the model, including axial thermal elongation E, thermal yaw angle error θ_x on *XZ* plane, and thermal pitch angle error θ_y on *YZ* plane. The input vector is $T = (T_1, T_5, T_6, T_7, T_{10})$, and ψ is neuron weight matrix, $T \to P$ is the transfer mapping function.

5.1. Model Structure

Setting a desired target, the efficiency of learning and iterations, the trainlm algorithm is used to train the network. Figure 9 illustrates the model structure; the hidden contains two layers of neurons, made up of 5 * 1 neurons. The network constitutes 5 input temperature variables, 3 output thermal drifts variables.
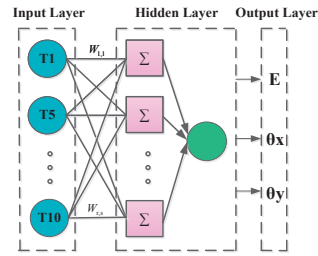

Fig. 9. Neural network structure

5.2. Model output

The experimental data in Figure 4 is as the training sample, and build the neural network model. The comparisons between predicted and experimental values are shown in Figure 10-12. The average absolute value of the residuals of axial thermal error E, radial thermal yaw angle θ_x and thermal pitch angle θ_y were 1.35μm, 1.56 " and 1.55" respectively, and the root squared mean error (RSME) is respectively of 2.98, 3.99 and 4.09. Moreover, predictive ability of the three thermal drifts was 94.6 %, 84.4 %, and 84.5 %, which indicate that the predictive power of the model is good.
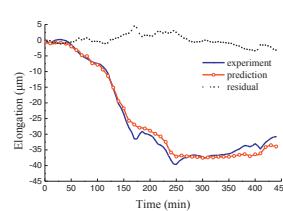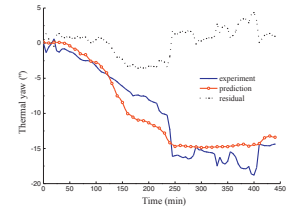

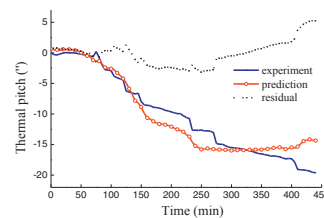Fig. 10. Axial thermal elongation   Fig. 11. Radial thermal yaw angle

Fig. 12. Radial thermal pitch angle

6. Model validation

To verify the validity of the model, the new data samples were used to predict the spindle thermal errors. Figure 13 describes the spindle speeds map corresponding to the new data samples.
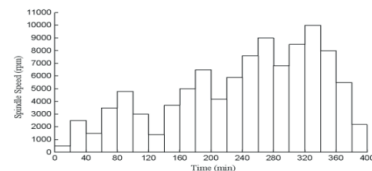

Fig. 13. Stochastic spindle speeds distribution

Figure 14-16 compares the model predictions with the measured values using Equation (9). The average absolute value of the residuals of axial thermal error E, radial thermal yaw angle θ_x and thermal pitch angle θ_y were 2.47μm, 1.34 " and 1.59" respectively. Moreover, predictive ability of the three thermal drifts was 90%, 88.8% and 87.2%, indicating the model has a good predictive ability and perfect generalization.
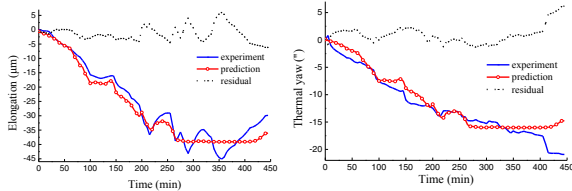
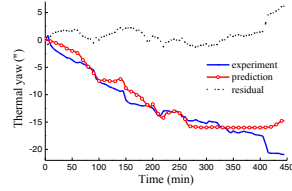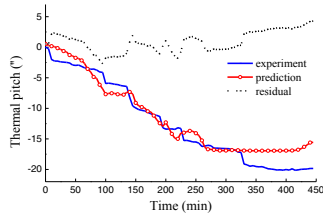Fig. 14. Axial thermal elongation   Fig. 15. Radial thermal yaw angle

Fig. 16. Radial thermal pitch angle

7. Conclusions

In this paper, using fuzzy clustering analysis method to group and optimize the temperature variables, and spindle axial / radial thermal errors ANN model is established, then the following conclusions can be reached.

(1) The Neural Network thermal error model based on fuzzy clustering pre-processing has an ability to predict precisely, and it is strong in generalization also. In addition, the model could be used for thermal error compensation technology to improve the precision of coordinate boring machine.

(2) The method of correlation analysis is used to optimize temperature variables, reducing the number of independent variables in modeling, and it can reduce modeling costs effectively. Furthermore, it also reduces the costs of thermal error compensation.

(3) The spindle thermal drifts include an axial thermal elongation, radial thermal yaw angle error and the radial thermal pitch angle error, and a unified multi-input multi-output predictive model can be established by the neural network. Moreover, the unified model makes it easy to implement the compensation of thermal error in the coordinate boring machine.

Acknowledgments

References

[1] Bryan J. International status of thermal error research. Annals of CIRP 1968; 16/1: 203-215.

[2] Yun Z, Xuesong M, Mingping S, Muxun X. An improved holospectrum-based balancing method for rotor systems with anisotropic stiffness. Proceedings of the Institution of Mechanical Engineers, Part C: Journal of Mechanical Engineering Science 2013; 227/2: 246-260.

[3] Mou J. A method of using neural networks and inverse kinematics for machine tool error estimation and correction. ASME Trans Journal of Manufacturing Science and Engineering 1997; 119:247-254.

[4] Donmez M.A, Hahn M.H, Soons J.A. A Novel Cooling System to reduce thermally-induced errors of machine tools, Annals of CIRP 2007; 56/1: 521–524.

[5] Min X, Jiang S. A thermal model of a ball screw drives system for a machine tool. Journal of Mechanical Engineering Science 2011; 1: 186-225.

[6] Haitao Z, Jianguo Y, Jinhua S. Simulation of thermal behavior of a CNC machine tool spindle. International Journal of Machine Tools and Manufacture 2007; 47/6: 1003–1010.

[7] Creighton E, Honegger A, Tulsian A, Mukhopadhyay D. Analysis of thermal errors in a high-speed micro-milling spindle. International Journal of Machine Tools and Manufacture 2010; 50 /4: 386–393.

[8] Rumelhart D E, Hinton G E, Williams R J. Learning representations of back-propagation errors. Nature (London) 1986; 323: 533-536.

[9] Yang S, Yuan J, Ni J. The improvement of thermal error modeling and compensation on machine tools by CMAC neural network. International Journal of Machine Tools and Manufacture 1996; 36 /4: 527-537.

[10] Chen J S. Fast calibration and modeling of thermally-induced machine tool errors in real machining. International Journal of Machine Tools and Manufacture 1997; 35/2: 159-169.

[11] Yi Z, Jianguo Y, Hui J. Machine tool thermal error modeling and prediction by grey neural network. International Journal of Advanced Manufacturing Technology 2012; 59/9: 1065-1072.

[12] Ouafi Abd E, Guillot M, Barka N. An integrated modeling approach for ANN-based real-time thermal error compensation on a CNC turning center. Advanced Materials Research, Environmental and Materials Engineering 2013; 664: 907-915.

[13] Hong Ce, Ibaraki So. Observation of thermal influence on error motions of rotary axes on a five-axis machine tool by static R-test. International Journal of Automation Technology 2012; 6/2: 196-204.

[14] Vyroubal Jiri. Compensation of machine tool thermal deformation in spindle axis direction based on decomposition method. Precision Engineering 2012; 36/1: 121-127.

[15] Vissiere A, Nouira H, Damak M, Gibaru O, David J.M. A newly conceived cylinder measuring machine and methods that eliminate the spindle errors. Measurement Science and Technology 2012; 23/9.

[16] ISO 230-3 Test code for machine tools Part 3: Determination of thermal effects, 2007:20-24.

[17] Ruspini E H. A new approach to clustering. Information and control 1969; 15/1: 22-32.

[18] Leahy R, Wu Z. An optional graph theoretic approach to data clustering: theory and its application to image segmentation. IEEE Trans on PAMI 1993; 15/11: 1101-1113.